Appl. Phys. A (2015) 119:75–83
DOI 10.1007/s00339-014-8959-1

Applied Physics A
Materials Science & Processing

Fabrication of superhydrophobic copper surface with excellent corrosion resistance

Libang Feng · Libin Zhao · Xiaohu Qiang · Yanhua Liu · Zhiqiang Sun · Bei Wang

Received: 12 October 2014 / Accepted: 16 December 2014 / Published online: 28 December 2014

Abstract This article presents an effective and facile method for preparing the superhydrophobic copper surface with excellent corrosion resistance. The superhydrophobic copper surfaces were fabricated by oxidizing, heat-treating, and alkyl chains' grafting. The resulting copper plates take on the binary structure which is composed of a great deal of nanosheets and needle-like/rod-like fibers. Just grounded on both the micro- and nanoscale hierarchical surface and the grafted long alkyl chains, the resulting copper plates are endued with the excellent water repellence, while the water contact angle and sliding angle can reach 157.3° and 5°, respectively. As a result, the superhydrophobic copper plates get the outstanding corrosion resistance.

1 Introduction

Wettability is one of the primary surface properties of solid materials, which is normally characterized by measurement of the contact angle of a surface [1–3]. Generally, surfaces with water contact angles larger than 150° and slide angles lower than 10° are called superhydrophobic surfaces [4, 5]. Nowadays, most of the researchers have focused on the fabrication of biomimetic superhydrophobic surfaces due to their potential applications in many fields, such as oil–water separation, anti-reflection, anti-adhesion, anti-sticking, anti-contamination, self-cleaning, and fluidic drag reduction [6].

L. Feng (✉) · L. Zhao · X. Qiang · Y. Liu · Z. Sun · B. Wang
School of Mechatronic Engineering, Lanzhou Jiaotong University, Lanzhou 730070, China
e-mail: lepond@hotmail.com

Copper is an important metal material used in many industrial fields and our daily life [7, 8]. Superhydrophobicity can endow the copper with special properties, such as anti-frosting, anti-corrosion, and minimizing the resistance to flow in microfluidic devices [9]. Thus, the superhydrophobic coppers have greater potential applications even under some rigorous environment [10, 11]. A variety of methods have been developed for the fabrication of many artificial superhydrophobic copper surfaces. For example, Guo and Yuan et al. [7, 9] mimicked the lotus leaf to fabricate superhydrophobic copper surfaces, respectively. Barthwal et al. [6] developed a facile method for fabrication of copper oxide hierarchical structure on copper substrate by the oxidation of copper in hot alkaline solutions. Many other techniques, such as electrochemical deposition [12, 13], graft polymerization [14], and sol–gel method [15–17], have been proposed to generate superhydrophobic surfaces on copper in recent years. However, most of the techniques described above require special equipment, multiple steps, specific substrates, or harsh chemical treatment, which seriously hinder the application of the fabrication methods in practice. Thus, it becomes the urgent demand of preparing the superhydrophobic copper surfaces by a simple and inexpensive method, and it will further greatly advance the application of the superhydrophobic coppers.

In this paper, we demonstrate a simple and low-cost technique for the fabrication of the superhydrophobic copper via creating copper oxide nanosheets structure on the copper plate and then modifying the resulting surface with stearic acid (STA). The whole procedure is simple to carry out, and no special equipment is required. Moreover, the method is also environment-friendly and inexpensive, while the as-fabricated superhydrophobic copper surface has excellent corrosion resistance.

2 Materials and methods

2.1 Materials

Copper plates (20 mm × 10 mm × 0.5 mm) and STA were purchased from Sinopharm Group Chemical Reagent Co., Ltd. HNO_3, NaOH, $(NH_4)_2S_2O_8$, and ethanol were purchased from Tianjin Benchmark Chemical Reagent Co., Ltd. (China).

2.2 Fabrication of the superhydrophobic copper surface

The superhydrophobic copper surface was prepared as shown in Scheme 1. Firstly, the copper plate was cleaned ultrasonically with dilute nitric acid (0.5 wt%) and deionized water, respectively, and then dried at room temperature. Second, the cleaned copper plate was dipped into 50 mL of NaOH (2.5 mol/L) and $(NH_4)_2S_2O_8$ (0.13 mol/L) solution at 60 °C for 20 min and then cleaned with deionized water and ethanol. Third, the resulting copper plate was heated at 180 °C for 2 h. Finally, the copper plate was immersed in 20 mmol/L of STA in ethanol for certain time and then cleaned with ethanol for three times.

2.3 Characterization

The water contact angle (CA) was measured with 10 μL of deionized water droplet at room temperature using a horizontal microscope with a protractor eyepiece (DSA 100, Kruss, Germany). At least five parallel measurements were made for each sample, and the value of average contact angles is reported. The sliding angle was measured by tilting the sample stage and recorded when the water droplet began to move in the downhill direction.

The surface morphology of the sample was observed with a field emission type of scanning electron microscopy (FE-SEM, JSM-6701F, Japan).

The phase and chemical structures were determined by X-ray diffractometry (XRD-7000, Shimadzu, Japan) and Fourier transform infrared spectroscopy (FT-IR, VER-TEX 70, Bruker, Germany), respectively. The powder scraped from the copper plate surface was examined in our measurement, and it can reflect the phase and chemical structure at the copper plate surface.

The polarization curve of electrochemical experiment was obtained with a computer-controlled electrochemical workstation (CHI660D, CH Instruments Inc) in 3.5 wt% of NaCl solution at room temperature.

3 Result and discussion

3.1 Morphology and wettability at the copper plate surface after different treatment steps

In order to fabricate a superhydrophobic surface on copper plate, a novel method was designed which includes two key processes. The first process is to prepare nanometer CuO rough structure on copper plate by oxidation of the copper plate with $(NH_4)_2S_2O_8$–NaOH and then treat at 180 °C. In the second process, the nanometer CuO film is modified by the low surface energy material of STA.

The surface morphology and a photograph of water droplet wetting at the copper plates in each step were investigated with SEM and digital camera, respectively, and results are shown in Fig. 1. It can be found that the surface of the cleaned copper plate is smooth and plain, while the water droplet spreads on the cleaned copper plate (as shown in Fig. 1a). After oxidized by $(NH_4)_2S_2O_8$, the morphology of the copper plate surface changes markedly, as shown in Fig. 1b. In specific, a rough surface with uniformly distributed nanosheets and needle-like/rod-like fibers appears on the copper plate surface, and the thickness of the nanosheets is 10–20 nm. Meanwhile, the water droplet spreads and wets the surface more easily, indicating that the oxidized copper surface is more hydrophilic. The heat treatment of the oxidized copper plate at 180 °C almost has no effect on the morphology, as shown in Fig. 1c. However, the wettability of the water droplet on the surface becomes worse than that of before heat treatment. Figure 1d shows the surface morphology of copper surface that further modified by STA. As compared to the

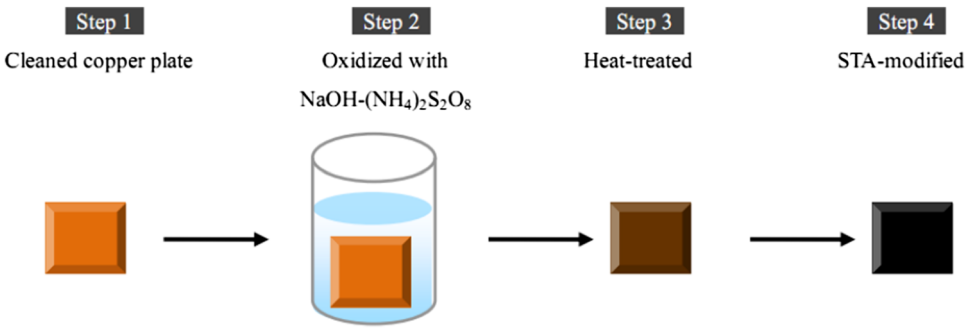

Scheme 1 Schematic procedure for fabricating the superhydrophobic copper surface

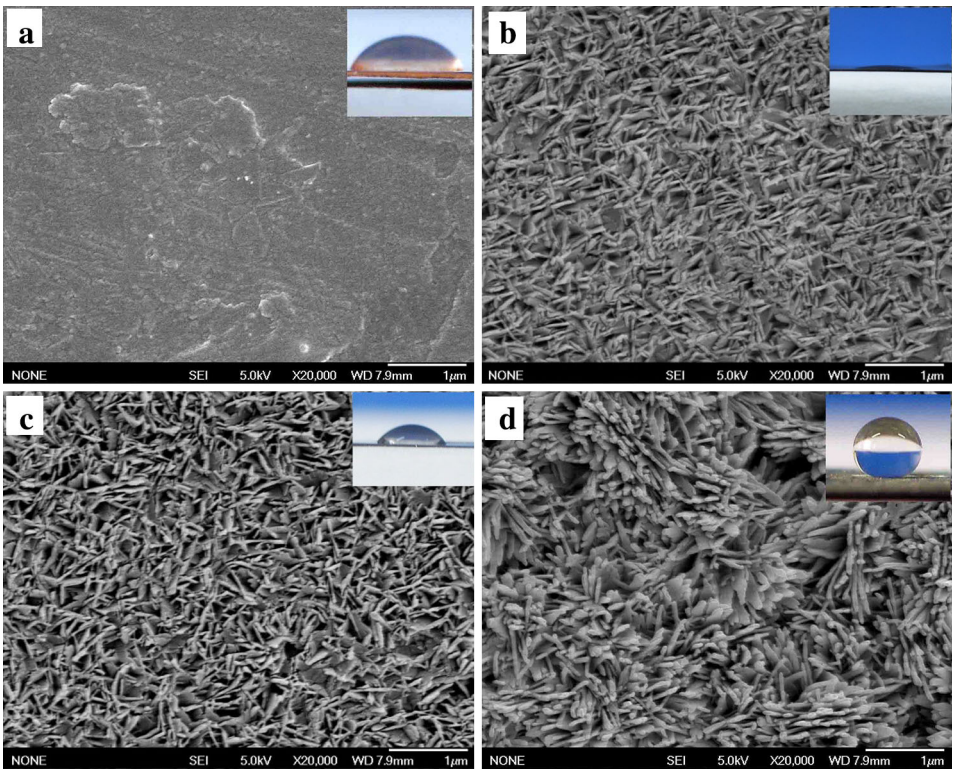

Fig. 1 SEM micrographs of the copper plate surfaces after different treatment steps: **a** cleaned, **b** oxidized, **c** heated at 180 °C, and **d** STA modification. The *insert* images show the shape of a water droplet on the corresponding surface

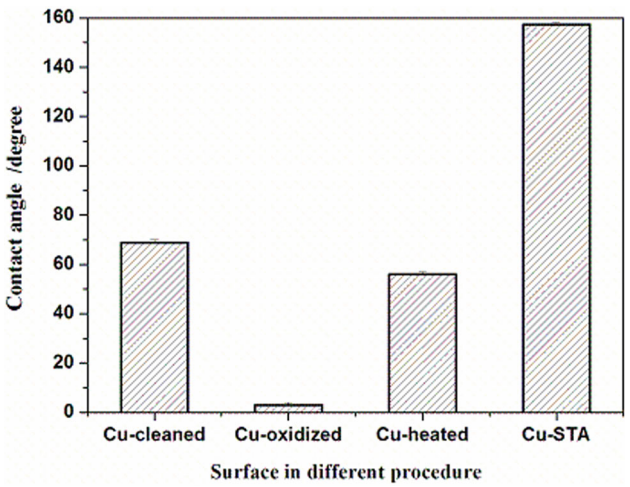

Fig. 2 Wettability of copper plate surfaces after different treatment steps

surface morphology before STA modification (see as Fig. 1c), it can be found that the rough structure changes to beautiful flower-like micro-clusters which consists of both nanosheets and needle-like/rod-like fibers. More importantly, the thickness of the nanosheets increases due to the STA grafting. Meanwhile, the water droplet settles on the surface with spherical shape, manifesting the resulting copper surface takes on strong hydrophobicity.

Then, the water contact angle at the copper plate surfaces after different treatment steps was investigated, and results are shown in Fig. 2. It can be found that the water contact angle at the cleaned copper plate is ca. 68.9°, while it decreases to about 3° after the cleaned copper plate was oxidized, indicating the copper plate surface takes on superhydrophilicity at this moment. However, the water contact angle increases to about 56.2° once again after the oxidized copper was heat-treated, while it further reaches 157.3° with very small sliding angle (ca. 5°) upon STA modification, showing that the copper plate gains excellent water repellence now.

The hydrophobicity and superhydrophobicity of the different surfaces provide an opportunity for further understanding the relationship between the surface wettability and the morphology.

According to Wenzel's equation [18]:

$$\cos\theta_r = r\cos\theta \tag{1}$$

where θ_r and θ denote the contact angle of a liquid droplet on a rough surface and a smooth solid surface made of the same materials, respectively, while r is the roughness factor which reflects the solid surface roughness. This equation indicates that the surface roughness enhances the hydrophilicity of a hydrophilic surface, while it increases the hydrophobicity of a hydrophobic surface because r is always larger than one. Since the surface roughness of the copper plate surface increases greatly after the oxidation (see as Fig. 1b), the water contact angle decreases outstandingly. Consequently, the copper plate surface takes on

the superhydrophilicity. However, the water contact angle increases to about 56° once again upon heat treatment, while the roughness has no much change before and after heat treatment, as can be seen from Fig. 1b, c.

Combining results from both Figs. 1 and 2, it can be deduced that the possible mechanism that leads to the typical structure and wettability above is as follows: First, the Cu plate is rapidly oxidized to Cu^{2+} in an alkaline oxidant solution, just as in alkaline solution of $(NH_4)_2S_2O_8$ in our research. Then, the highly alkaline conditions favor the square planar coordination of OH^- groups to Cu^{2+}, which leads to an extended chain along a crystal face and forming a 2D structure. Finally, the 2D $Cu(OH)_2$ layers are stacked through the relatively weak hydrogen bond interactions to forma 3D structure, just as nanosheets in Fig. 1b. The structure of $Cu(OH)_2$ is unstable. Consequently, the interplanar hydrogen bonds will be broken at 180 °C for 2 h, and the cleavage of the interplanar hydrogen bonds causes the $Cu(OH)_2$ nanosheets to crack into pieces of CuO sheets/ribbons [19–21]. The formation procedure of CuO is shown in Scheme 2, and the corresponding chemical reactions are as follows:

$$Cu + 2NaOH + (NH_4)_2S_2O_8 \rightarrow Cu(OH)_2 + (NH_4)_2SO_4 + Na_2SO_4$$

$$Cu(OH)_2 \rightarrow CuO + H_2O$$

The amount of the hydroxyl groups at the copper plate surface decreases when $Cu(OH)_2$ decomposes into CuO as a result of dehydration reaction. Consequently, the water contact angle enhances after heat treatment. Next, the contact angle increases remarkably after STA modification. The Cassie and Baxter model [22] is applied here to describe the CA of a superhydrophobic surface with low hysteresis,

$$\cos\theta_r = f_1 \cos\theta - f_2 \quad (2)$$

where θ_r and θ denote the contact angle of a liquid droplet on a rough surface and a smooth solid surface made of the same materials, respectively, while f_1 and f_2 are the fractional areas estimated for the solid and the air trapped between STA-modified copper plate surface and a water droplet, respectively (i.e., $f_1 + f_2 = 1$). This equation indicates that the larger the air fraction (f_2), the more hydrophobic the surface. In our study, the rough structure with flower-like micro-clusters forms after the STA modification, and the micro flower-like aggregates, which consists of both nanosheets and needle-like/rod-like fibers, can trap more air. In our experiment, the resulted θ_r is 157.3° while θ at the flat copper after alkyl chains' grafting is 88.1°. So, the calculated f_2 in our system is 0.9235, which indicates that a large quantity of air is trapped when the copper plate surface is in contact with water. Therefore, the achievement of the superhydrophobicity at the copper surface is a result of both the rough structure and the modification of the hydrophobic materials, which successfully prevents the penetration of the water into the interspaces among nanosheets and needle-like/rod-like fibers.

3.2 Phase structure of the copper plate after different treatment steps

The phase structure of the copper plate in each step was analyzed by XRD technique, and the investigated XRD patterns are shown in Fig. 3. It can be seen from the XRD pattern of the cleaned copper plate (see as Fig. 3a) that three main diffraction peaks present at 2θ of 43.6°, 50.7°, and 74.4°. These crystal peaks are ascribed to the cubic copper phase with orientation planes of (111), (200), and (220), respectively, which are well in agreement with the JCPDS file No. 85-1326 of the copper metallic particles. The XRD pattern of the copper plate after oxidized also shows three main diffraction peaks at the same diffraction degrees. More importantly, new peaks at 2θ of 36.5° and 38.8° appear, as shown in Fig. 3b. The 2θ value is indexed to the corresponding crystal plane as the JCPDS file No. 78-0428, and it is affirmed that the new peak belongs to CuO nanosheets with orientation plane of (002) and (111). By contrast, the XRD pattern of the heat-treated copper plate (see as Fig. 3c) has no evident change as compared to that of the oxidized copper plate. Additionally, as compared to the heat-treated copper plate, the XRD pattern of the copper plate upon STA modification (see as Fig. 3d) is not change any more, indicating that STA graft has no influence on the phase structure of the copper plate.

3.3 Effect of STA modification on the chemical structure

The contact angle increases to 157.3° after the copper plate surface is modified with STA, suggesting that the surface chemical composition plays a significant role on the wettability. Thereupon, the chemical structure at the copper plate surface before and after STA modification was analyzed with FT-IR technique, and the resulting spectra are shown in Fig. 4. In order to compare

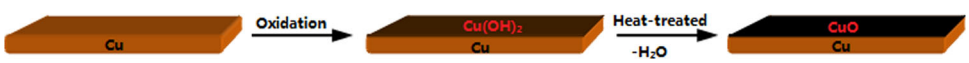

Scheme 2 Formation procedure of CuO nanosheets

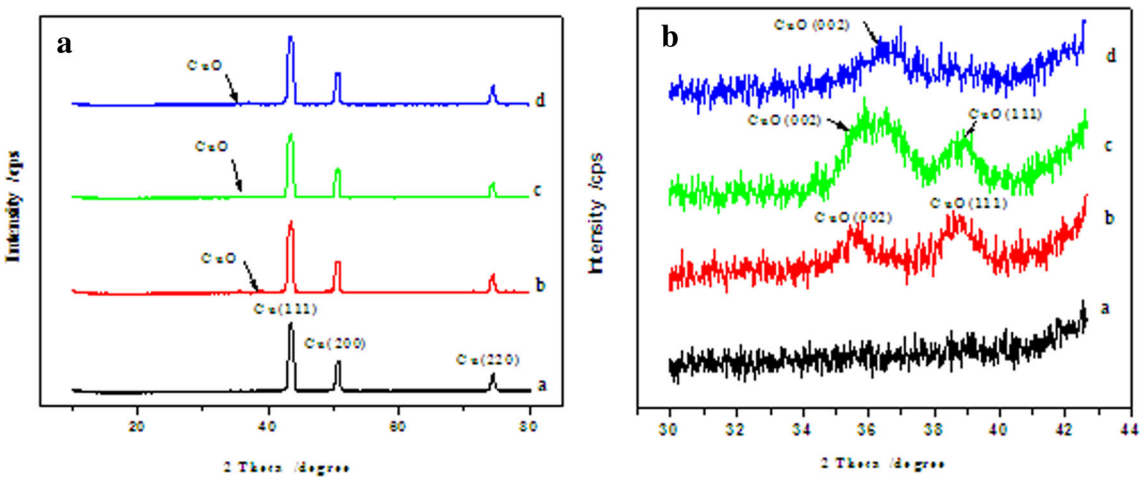

Fig. 3 X-ray diffraction patterns of the copper plates: (*a*) cleaned, (*b*) oxidized, (*c*) heat-treated, (*d*) STA modified

conveniently, the infrared spectrum of STA is included as Fig. 4c as well.

Figure 4a shows IR spectrum of the copper plate surface before STA modification. The wide peak centered at 3,440 cm^{-1} is assigned to the stretching vibration absorption of Cu–OH. By contrast, great changes happen in IR spectrum of the copper plate surface after STA modification, as shown in Fig. 4b. Referring to the IR spectrum of STA, it can be found that the absorption of –COOH group presenting at 1,706 cm^{-1} from free STA molecules (see Fig. 4c) moves to 1,645 cm^{-1} for the copper plate surface modified with STA [23] (as shown in Fig. 4b). Meanwhile, a new adsorption peak at 1,526 cm^{-1} presents, which stems from the stretching vibration of $–COO^-$ groups. These results indicate that the chemical reaction between carboxyl groups in STA and Cu–OH at the copper plate surface takes place successfully. Additionally, a new absorption peak of the symmetric bending of $–CH_2–$ groups also presents at 1,460 cm^{-1}, while the symmetric and asymmetric stretching vibration of $–CH_2–$ groups still appear at 2,920 and 2,850 cm^{-1}, respectively. Based on the FT-IR analysis, it can be deduced that the chemical reaction between Cu–OH and STA really happens, and the reaction mechanism may be as follows.

$$Cu-OH + CH_3(CH_2)_{16}COOH \rightarrow CH_3(CH_2)_{16}COO-Cu + H_2O$$

Thus, it can be concluded that $CH_3(CH_2)_{16}COO–Cu$ forms at the copper plate surface after STA modification, and the water-repellent long alkyl chains (namely, $C_{17}H_{35}COO^-$) are chemically bonded onto the copper plate surface successfully.

3.4 Effect of STA immersion time on the wettability

To clarify whether the STA modification time affects the superhydrophobicity of the as-prepared copper plate, the

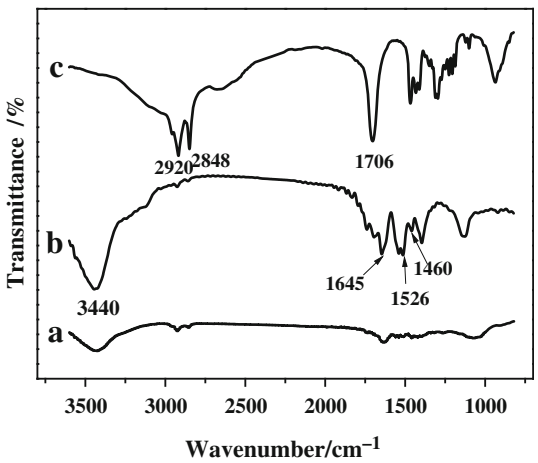

Fig. 4 FT-IR spectra of the copper before (*a*) and after (*b*) STA modification together with the stearic acid (*c*)

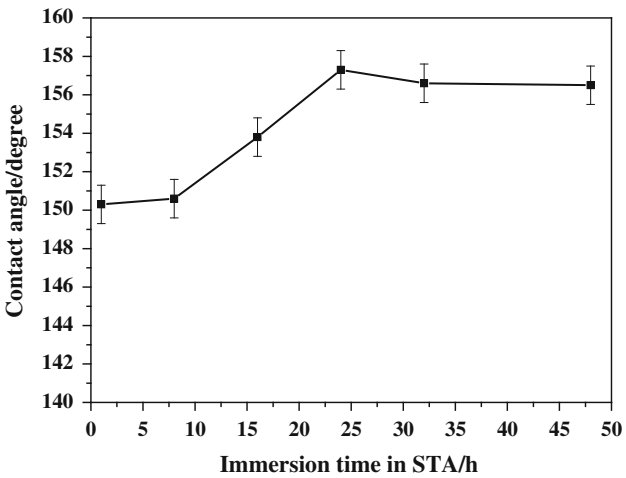

Fig. 5 Water contact angle on the copper surface vs the treatment time in STA–ethanol solution

immersion time in STA–ethanol solution on the water contact angle (CA) was investigated, and the change trend of the contact angle with the STA–ethanol immersion time is shown in Fig. 5. It can be found that CA increases gradually with the extension of the immersion time before 24 h. Thereafter, CA decreases appreciably with the treatment time further increase. Such phenomenon can be explained in terms of Cassie–Baxter equation (see as Eq. 2), too. When treated in STA–ethanol solution less than 24 h, the hydrophobic alkyl chains (namely, $C_{17}H_{35}COO^{-}$) can chemically graft onto the copper surface. With the extension of the immersion time reaches 24 h, more STA molecules are grafted increasingly. As a result, more and more air is trapped in the solid–liquid contact area when the water droplet is applied. Consequently, the CA gets the highest value of 157.3°. On the contrary, if the STA treatment time is too long (in this research, more than 24 h), the amount of the grafted STA molecules becomes saturated. Thereupon, some STA molecules may deposit on the copper surface in the form of physical adsorption, while some physically adsorbed STA molecules cannot be washed away by alcohol under ultrasonification. So as a result, the CA decreases appreciably due to the –COOH in STA molecules has hydrophilic property.

3.5 Microstructure and the water repellence of the superhydrophobic copper surface

The modification with STA not only changes the surface chemistry, but also influences the morphology of the copper surface. Figure 6 shows SEM images with the different magnifications of the STA-modified copper surface.

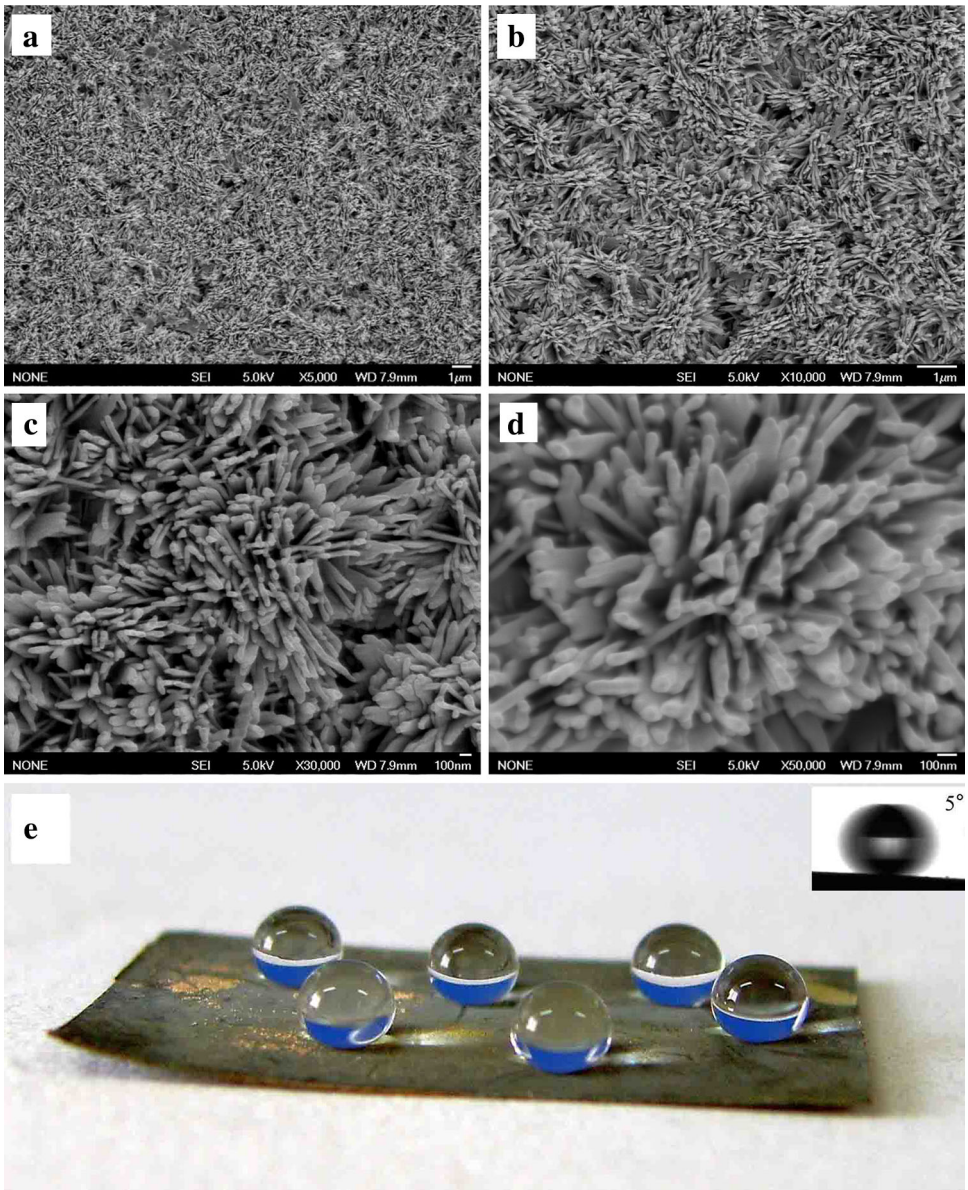

Fig. 6 SEM micrographs of the superhydrophobic copper surface with different magnifications (**a**–**d**), and the image of water droplets on the superhydrophobic copper substrate (**e**). The *insert* shows a photograph of a water droplet with a sliding angle of 5°

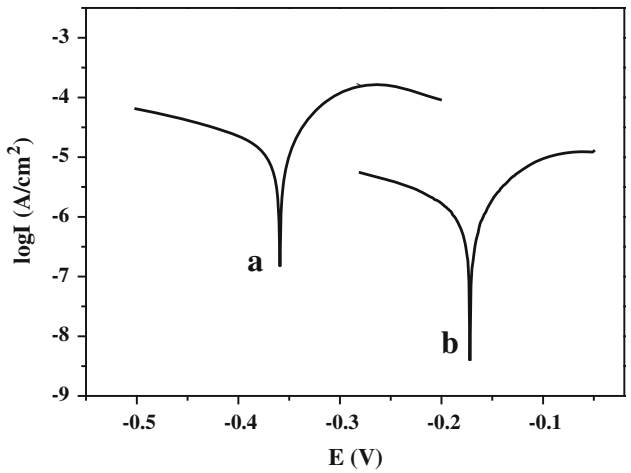

Fig. 7 Polarization curves for copper plates in 3.5 wt% of NaCl solution: (*a*) blank, (*b*) the superhydrophobic sample

Meanwhile, the digital photograph of water droplets on a superhydrophobic copper substrate together with the corresponding photograph of a droplet with a sliding angle of 5° is listed in Fig. 6.

It can be found from Fig. 6a that even surface presents in the micrograph, while the surface is composed of a great deal of straw-like structure. The higher magnification micrograph (see Fig. 6b) shows that the even copper surface consists of lots of 3D flower-like micro-clusters. The further magnified micrograph (see as Fig. 6c, d) shows that each cluster is composed of many nanosheets and needle-like/rod-like fibers, and most nanosheets and fibers arrange perpendicular to the copper surface. Consequently, the flower-like hierarchical porous surface with a mass of channels or interspace is formed. The diameter of the needle-like/rod-like fiber is 15–25 nm, while the width of the channel is between 50 and 200 nm, which indicates that the resulting superhydrophobic copper surface has binary morphology with both micro- and nanoscale structure.

Just grounded on both the micro- and nanoscale hierarchical structure and the water-repellent long $C_{17}H_{35}$-COO– alkyl chains, the resulting copper plate takes on the excellent superhydrophobic property. Thus, the water droplet settles on the resulting copper surface with spherical shape, as shown in Fig. 6d. Meanwhile, a large quantity of air is trapped in the channels/interspace among nanosheets and fibers. Consequently, the resulting copper surface possesses both higher water contact angle and lower sliding angle.

Table 1 The corrosion potential (E_{corr}) and the corrosion current density (I_{corr}) of the blank copper and the superhydrophobic copper in 3.5 wt% NaCl solution

Sample	E_{corr} (V)	I_{corr} (A cm^{-2})
Blank copper	−3.60	5.248×10^{-5}
Superhydrophobic copper	−1.75	5.623×10^{-6}

3.6 Corrosion resistance and mechanism of the superhydrophobic copper

The corrosion behavior of superhydrophobic copper plates was evaluated by the Tafel extrapolation method in 3.5 wt% of NaCl aqueous solution. The obtained potentiodynamic polarization curves is shown in Fig. 7, while the corrosion potential (E_{corr}) and corrosion current density (I_{corr}), which are derived from Fig. 7, are listed in Table 1.

It can be found from Fig. 7 and Table 1 that the E_{corr} of the blank copper plate is −3.60 V. By contrast, the E_{corr} of the superhydrophobic copper plate increases to −1.50 V. Meanwhile, the I_{corr} of the blank and superhydrophobic copper plate are 5.248×10^{-5} and 5.623×10^{-6} A·cm^{-2}, respectively, indicating that the corrosion current density decreases by one order of magnitude when the copper plate surface gets the superhydrophobicity. Generally, a lower corrosion current density or a higher corrosion potential corresponds to a lower corrosion rate and a better corrosion resistance [24]. Therefore, it can be seen that as compared

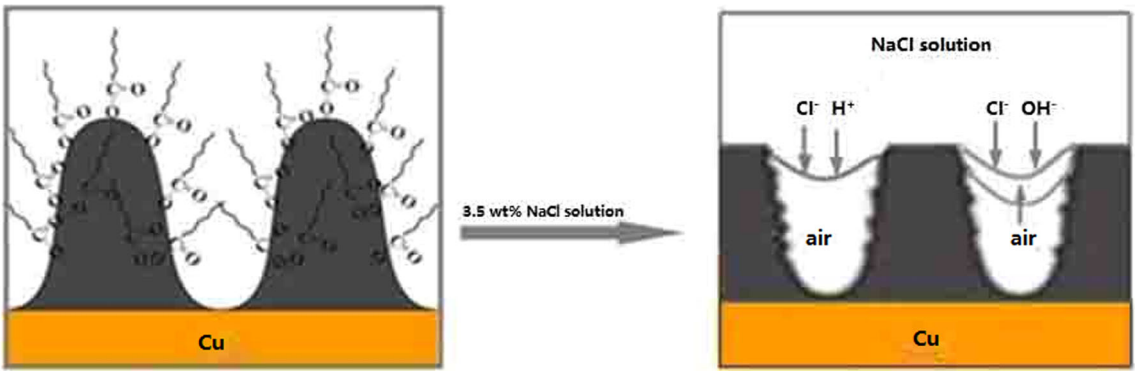

Fig. 8 Model of the interface between superhydrophobic copper surface and 3.5 wt% NaCl solution

to the blank copper plate, the superhydrophobic copper plate possesses a higher chemical stability and corrosion resistance. These results indicate that the corrosion resistance of the copper plate has been improved greatly when the copper surface is endowed with superhydrophobicity [25, 26].

Both the increase of the E_{corr} and the decrease of I_{corr} for the superhydrophobic copper plate can be well explained by 'Cushion Effect' and 'Capillarity' [25–27]. Figure 8 shows the schematic illustration of the possible microstructure and micro-model at the interface of the superhydrophobic copper surface in contact with the NaCl solution. The superhydrophobic surface composed of micro-protrusions and the hydrophobic alkyl chains. The hierarchical structure surface can easily trap a great deal of air at the interface. Therefore, an effective barrier obtains so as to further block the water and the corrosive Cl^- to enter and contact with the copper surface, which further prevent the superhydrophobic copper surface from corrosion due to oxygen and water caused by the electrochemical reaction. As a result, the corrosion rate of the superhydrophobic copper decreases greatly as compared to the untreated copper. Consequently, the corrosion resistance of the copper is improved. Therefore, the superhydrophobic copper can be protected perfectly in the brine and seawater.

4 Conclusions

In summary, an effective and facile method for preparing the superhydrophobic copper surface with excellent corrosion resistance has been developed. The resulting copper surfaces present a high water contact angle of 157.3° and a low sliding angle of <5°. The SEM image and XRD patterns of the oxidized and heat-treated copper plates show rough morphology composed of nanosheets due to the formation of CuO. After modified by STA, the long hydrophobic alkyl chains are chemically grafted onto the porous copper surface. Consequently, the hierarchical surface with beautiful flower-like micro-clusters is resulted, while clusters are composed of a great deal of nanosheets and needle-like/rod-like fibers. Grounded on both the micro- and nanoscale hierarchical structure and the grafted water-repellent long $C_{17}H_{35}COO$– alkyl chains, the resulting copper plate takes on the excellent superhydrophobic property. As a result, the copper plate endues with excellent corrosion resistance when the copper surface has superhydrophobicity.

The present work provides a simple and systemic condition for fabricating flower-like superhydrophobic copper surfaces with excellent corrosion resistance. Moreover, it further explores to create multifunctional materials having superior properties like self-cleaning, anti-icing, anti-frosting, and so forth.

Acknowledgments This research is supported by National Natural Science Foundation of China (Grant No. 21161012).

References

1. T.P. Nguyen, R. Dufour, V. Thomy, V. Senez, R. Boukherroub, Y. Coffinier, Fabrication of superhydrophobic and highly oleophobic silicon-based surfaces via electroless etching method. Appl. Surf. Sci. **295**, 38 (2014)
2. C.F. Wang, W.Y. Chen, H.Z. Cheng, Pressure-proof superhydrophobic films from flexible carbon nanotube/polymer coatings. J. Phys. Chem. C **37**, 15607 (2010)
3. Y.L. Zhang, J.N. Wang, Y.Y. He, B.B. Xu, S. Wei, F.S. Xiao, Solvothermal synthesis of nanoporous polymer chalk for painting superhydrophobic surfaces. Langmuir **27**, 12858 (2011)
4. M.N. Valipour, F.C. Birjandi, J. Sargolzaei, Super-non-wettable surfaces: a review. Colloid Surf. A **448**, 93 (2014)
5. L. Cao, T.P. Price, M. Weiss, Super water-and oil-repellent surfaces on intrinsically hydrophilic and oleophilic porous silicon films. Langmuir **24**, 1640 (2008)
6. S. Barthwal, Y.S. Kim, S.H. Lim, Superhydrophobic and superoleophobic copper plate fabrication using alkaline solution assisted surface oxidation methods. Int. J. Precis. Eng. Manuf. **13**, 1311 (2012)
7. L.B. Feng, H.X. Zhang, P.Z. Mao, Superhydrophobic alumina surface based on stearic acid modification. Appl. Surf. Sci. **257**, 3959 (2011)
8. S. Yuan, S.O. Pehkonen, B. Liang, Y.P. Ting, K.G. Neoh, E.T. Kang, Superhydrophobic fluoropolymer-modified copper surface via surface graft polymerization for corrosion protection. Corros. Sci. **53**, 2738 (2011)
9. Z.Q. Yuan, X. Wang, A novel fabrication of a superhydrophobic surface with highly similar hierarchical structure of the lotus leaf on a copper sheet. Appl. Surf. Sci. **285**, 205 (2013)
10. N.J. Shirtcliffe, G. McHale, M.I. Newton, C.C. Perry, Wetting and wetting transitions on copper-based super-hydrophobic surfaces. Langmuir **21**, 937 (2005)
11. L. Huang, Z. Liu, Y. Liu, Y. Gou, Preparation and anti-frosting performance of super-hydrophobic surface based on copper foil. Int. J. Therm. Sci. **50**, 432 (2011)
12. M. Mahajan, S.K. Bhargava, P. Anthony, Electrochemical formation of porous copper 7,7,8,8-tetracyanoquinodimethane and copper 2,3,5,6-tetrafluoro-7,7,8,8-tetracyanoquinodimethane honeycomb surfaces with superhydrophobic properties. Electrochim. Acta **102**, 186 (2013)
13. R. Qiu, P. Wang, D. Zhang, J. Wu, One-step preparation of hierarchical cobalt structure with inborn superhydrophobic effect. Colloid Surf. A **377**, 144 (2011)
14. Y. Zhao, W. Yang, G. Zhang, Y. Ma, J. Yao, A hierarchical self-assembly of 4,5-diphenylimidazole on copper. Colloid Surf. A **277**, 111 (2006)
15. A.V. Rao, S.S. Latthe, S.A. Mahadik, C. Kappenstein, Mechanically stable and corrosion resistant superhydrophobic sol-gel coatings on copper substract. Appl. Surf. Sci. **13**, 5772 (2011)
16. C. Dong, Y. Gu, M. Zhong, L. Li, K. Sezer, M. Ma, W. Liu, J. Mater. Process. Technol. **211**, 1234 (2011)
17. Y. Fan, C. Li, Z. Chen, H. Chen, Study on fabrication of the superhydrophobic sol-gel films based on copper wafer and its anti-corrosive properties. Appl. Surf. Sci. **258**, 6531 (2012)

18. R.N. Wenzel, Surface roughness and contact angle. J. Phys. Org. Chem. **53**, 1466 (1949)
19. Q.B. Zhang, K.L. Zhang, CuO nanostructures: synthesis, characterization, growth mechanisms, fundamental properties, and applications. Prog. Mater Sci. **60**, 208 (2014)
20. W. Zhang, X. Wen, S. Yang, Controlled reactions on a copper surface: synthesis and characterization of nanostructured copper compound films. Inorg. Chem. **42**, 5005 (2003)
21. Q.B. Zhang, D.G. Xu, X. Zhou, In situ synthesis of CuO and Cu nanostructures with promising electrochemical and wettability properties. Small **5**, 935 (2014)
22. A.B.D. Cassie, S. Baxter, Wettability of porous surfaces. Trans. Faraday Soc. **44**, 546 (1944)
23. L.B. Feng, Y.H. Che, Superhydrophobic alumina surface based on stearic acid modification. Appl. Surf. Sci. **283**, 367 (2013)
24. W.J. Xu, J.L. Song, J. Sun, Rapid fabrication of large-area, corrosion-resistant superhydrophobic Mg alloy surfaces. ACS Appl. Mater. Inter. **3**, 4404 (2011)
25. J. Han, Q.J. Xu, G.L. Zhang, Effect of super-hydrophobic surface on the corrosion performance of copper and copper alloys. Adv. Mater. Res. **864**, 447 (2013)
26. P. Wang, D. Zhang, P. Ju, Super-hydrophobic film fabricated on copper with electro-deposition method and its corrosion resistance. Adv. Mater. Res. **803**, 278 (2013)
27. P. Wang, D. Zhang, R. Qiu, Green approach to fabrication of a super-hydrophobic film on copper and the consequent corrosion resistance. Corros. Sci. **80**, 366 (2014)